DOI: 10.1111/eci.12107

ORIGINAL ARTICLE

SFTPC mutations cause SP-C degradation and aggregate formation without increasing ER stress

Tobias Thurm, Eva Kaltenborn, Sunčana Kern, Matthias Griese[1] and Ralf Zarbock[1]

Dr. von Hauner Children's Hospital, Ludwig-Maximilians-University, Munich, Germany

ABSTRACT

Background Mutations in the gene encoding surfactant protein C (SP-C) cause familial and sporadic interstitial lung disease (ILD), which is associated with considerable morbidity and mortality. Unfortunately, effective therapeutic options are still lacking due to a very limited understanding of pathomechanisms. Knowledge of mutant SP-C proprotein (proSP-C) trafficking, processing, intracellular degradation and aggregation is a crucial prerequisite for the development of specific therapies to correct aberrant trafficking and processing of proSP-C and to hinder accumulation of cytotoxic aggregates.

Materials and methods To identify possible starting points for therapeutic intervention, we stably transfected A549 alveolar epithelial cells with several proSP-C mutations previously found in patients suffering from ILD. Effects of mutant proSP-C were assessed by Western blotting, immunofluorescence and Congo red staining.

Results A group of mutations (p.I73T, p.L110R, p.A116D and p.L188Q) resulted in aberrant proSP-C products, which were at least partially trafficked to lamellar bodies. Another group of mutations (p.P30L and p.P115L) was arrested in the endoplasmic reticulum (ER). Except for p.I73T, all mutations led to accumulation of intracellular Congo red–positive aggregates. Enhanced ER stress was detectable in none of these stably transfected cells.

Conclusions Different SP-C mutations have unique consequences for alveolar epithelial cell biology. As these cannot be predicted based upon the localization of the mutation, our data emphasize the importance of studying individual mutations in detail in order to develop mutation-specific therapies.

Keywords A549 cells, ER stress, interstitial lung disease, *SFTPC* mutations, surfactant protein C.

Eur J Clin Invest 2013; 43 (8): 791–800

Introduction

Surfactant protein C (SP-C) is a component of pulmonary surfactant, a mixture of lipids and proteins that reduces alveolar surface tension and is therefore indispensable for normal breathing and gas exchange [1,2]. Lamellar bodies are specific organelles for the storage and secretion of pulmonary surfactant in alveolar type II cells [3–6]. Surfactant secretion from mature lamellar bodies is accomplished by their fusion with the plasma membrane [7,8]. SP-C is encoded by the *SFTPC* gene, which is expressed exclusively in alveolar type II cells. The 21-kDa proprotein (proSP-C) consists of 197 amino acids and is proteolytically cleaved in four steps, yielding mature SP-C with a size of 3·7 kDa that comprises the amino acids 24–58 of proSP-C [7]. The C-terminus comprises a non-BRICHOS domain, reaching from His_{59} to Thr_{93}, and a BRICHOS domain from Phe_{94} to Ile_{197}.

Mutations in the *SFTPC* gene were the first molecularly defined genetic cause in the large and heterogeneous group of patients with sporadic and familial interstitial lung diseases (ILD) [9,10]. However, for the majority of ILD cases, the causative genes still remain unidentified [11]. All hitherto described *SFTPC* mutations have been found in a heterozygous state in affected individuals consistent with an autosomal dominant pattern of inheritance observed in familial cases [7,9,12]. Clinically, patients with *SFTPC* mutations either present with acute respiratory distress and early death in infancy or with chronic lung disease characterized by dyspnoea and hypoxaemia. Histologically, various patterns are found with no obvious relationship between *SFTPC* genotype and the clinical phenotype.

Little is known regarding the pathogenesis of ILD associated with *SFTPC* mutations. It has been suggested that SP-C mutations lead to the induction of ER stress [13], cytotoxicity [14]

[1]These authors contributed equally to this paper.

and caspase-mediated apoptosis [15–17]. However, it is not known whether these mechanisms are generally applicable or apply only to certain mutations. This is crucial because in case the mechanisms were different for distinct mutations, specific therapies had to be developed, based upon the actual features of each class of mutations. Therefore, the goal of this study was to determine the influence on SP-C trafficking, processing, intracellular degradation and aggregation of different clinically relevant mutations. Until 2009, p.P30L was the only mutation known localized in the mature SP-C protein [7]. Histopathological alterations include thickened alveolar septa, a hyperplastic alveolar epithelium and accumulation of alveolar macrophages [8]. In the C-terminal non-BRICHOS part of proSP-C, several mutations have been described [18–22]. Among these, p.I73T represents a mutational hot spot, accounting for about 30% of all SP-C mutations described [23]. Mutations located in the C-terminal BRICHOS domain have been suggested to primarily affect proper folding, trafficking and processing of proSP-C [7,15,16,24]. Several clinically relevant mutations in the BRICHOS domain have been examined so far, for example, p.A116D, p.L188Q and Δexon4 [9,10,18,25,26]. Apart from p.A116D and p.L188Q, which have been described previously to some extent [10,13,27,28], we focused on two mutations whose cellular biology has been barely investigated yet, namely p.L110R and p.P115L [7,9,12]. In children, these mutations were associated with interstitial pneumonitis, cough and respiratory distress. We found that all *SFTPC* mutations investigated herein caused altered intracellular SP-C degradation or aggregate formation without increasing ER stress.

Materials and methods

Plasmid vectors

For the expression of SP-C with N-terminal hemagglutinin (HA)-tag (HA^N-SP-C), hSP-C cDNA was cloned into a modified pUB6/V5-His vector, as previously described [29]. The SP-C point mutations were introduced into hSP-C cDNA by site-directed mutagenesis (QuickChange Site-Directed Mutagenesis Kit, Stratagene, La Jolla, CA, USA).

Cell culture

The human lung epithelial cell line A549 (ACC 107; DMSZ, Braunschweig, Germany) was stably transfected with HA^N-SP-C at 70% confluence using ExGen 500 (Fermentas, St. Leon-Rot, Germany). Transfected cells were selected using 6 μg/mL blasticidin (Invivogen, San Diego, CA, USA) and incubated for 14 days in 96-well plates. For immunoblotting, cells were grown in 6-well plates (10^6 cells/well) for 48 h prior to harvesting. For immunofluorescence and Congo red staining, cells were grown on cover slips in 12-well plates (10^5 cells/well) for 24 h and fixed in 4% paraformaldehyde.

Immunofluorescence

Immunofluorescence was performed using the following primary antibodies: anti-HA (Roche, Penzberg, Germany), anti-LAMP3/CD63 (Millipore, Schwalbach, Germany), anti-calnexin (Enzo Life Sciences, Lörrach, Germany), anti-EEA1 (Acris Antibodies, Herford, Germany), anti-ubiquitin (Biomol, Hamburg, Germany) and anti-GM130 (Santa Cruz Biotechnology, Santa Cruz, CA, USA). Signals were visualized using Alexa 488, Alexa 546 and Alexa 555 secondary antibodies (Invitrogen, Karlsruhe, Germany). Cells were mounted by Vectashield® with DAPI. Fluorescent signal was examined with an Axiovert 135 fluorescence microscope (Carl Zeiss, Jena, Germany). Quantification of colocalization was performed by counting HA dots and merge dots in the cells and calculation of the ratio of merge dots to HA dots.

Staining Congo red–positive aggregates

After growing, fixing and permeabilization, cultured cells were treated by 0·02% Congo red solution (80% ethanol, saturated NaCl, 1% NaOH) and dehydrated using increasing concentrations of ethanol. Cells were mounted with Rothi-Histokitt (Carl Roth, Karlsruhe, Germany). The fluorescence signal was examined using an Axiovert 135 fluorescence microscope.

Immunoblotting

Cultured cells were harvested with trypsin (PAA, Pasching, Austria) and resuspended in lysis buffer (0·15 M NaCl, 1% Triton-X100, 0·5% sodium deoxycholate, 50 mM Tris, 5 mM EDTA) with protease inhibitor complete (Roche). 30 μg of total protein was transferred to a PVDF membrane and immunoblotted using anti-HA (Roche), anti-LC3A/B (Cell Signaling, Danvers, MA, USA), anti-BiP/GRP78 (Cell Signaling) and anti-ß-actin HRP conjugate (Santa Cruz) as primary antibodies. HRP-conjugated secondary antibodies anti-rat IgG (Dako, Glostrup, Denmark) and anti-rabbit IgG (Dianova, Hamburg, Deutschland) were used. The chemiluminescence signal was detected by ECL Detection Reagent (GE Healthcare, Freiburg, Germany) and analysed by densitometry.

Immunoprecipitation

Hemagglutinin antibody was coupled to magnetic beads (Dynabeads; Invitrogen) overnight. Cultured cells were harvested and resuspended in lysis buffer, as described above. After proSP-C from lysates was precipitated by beads and collected in a new tube, precipitates were loaded to an immunoblotting gel, and proSP-C was detected by HA antibody as described.

Secreted Luciferase reporter assay

For luciferase assay, A549 cells stably expressing SP-C^{WT} or SP-C mutations were transfected together with p-MET-luc vector using ExGen500 (Fermentas). Luciferase activity (secretory level) was measured in cell supernatant 24 h later by photometry.

MTT assay

To measure cell viability and cytotoxicity of SP-C mutations, MTT (3-(4,5-Dimethylthiazol-2-yl)-2,5-diphenyltetrazolium bromide) assay was performed. For this assay, A549 cells stably expressing SP-C^{WT} or SP-C mutations were seeded in 96-well plates (1250 cells/well) and incubated for 48–72 h, followed by MTT/DMSO treatment and absorbance measurement using a spectrophotometer at wavelength 540 nm.

Real-time quantitative PCR

Total RNA was collected from cells grown for 48 h in T75 flasks using the High-Pure RNA Isolation Kit (Roche) according to the manufacturer's instructions. RNA concentrations were determined with a NanoDrop spectrophotometer (Thermo Scientific, Schwerte, Germany). One microgram of total RNA was transcribed into cDNA with the QuantiTect transcription kit (Qiagen, Hilden, Germany). Quantitative PCR was carried out on a 7900 HT PCR system (Applied Biosystems, Foster City, CA, USA) using SensiFAST SYBR Hi-ROX premix (Bioline, Luckenwalde, Germany) in 20 μl reaction volumes. Relative gene expressions were calculated using the $2^{-\Delta\Delta CT}$ method with *HPRT1* as housekeeper. Sequences of primers used were GGCCTCGTGGTGTATGAC (forward primer) and TGGCCCAGCTTAGACGTA (reverse primer) for *SFTPC* and CATTGTAGCCCTCTGTGTGC (forward primer) and CTGACCAAGGAAAGCAAAGTCTG (reverse primer) for *HPRT1*.

Statistical analysis

Statistical analyses were performed by one-way ANOVA and Dunnett *post hoc* test using SPSS 17.0 (SPSS Inc., Chicago, IL, USA) Results were presented as mean values ± SEM from a minimum of four experiments. *P*-values < 0·05 were considered significant.

Results

SFTPC mutations do not influence cellular viability and overall cell secretory capacity

Cell viability assessed using the MTT assay was not compromised by expression of proSP-C mutations (data not shown). To analyse whether overexpression of proSP-C leads to variations in the general secretory capacity of the cells, we assayed secretory activity using luminescence measurement of secreted luciferase activity. Overexpression of proSP-C^{WT} increased secretory activity compared with A549 cells. However, after normalizing to proSP-C mRNA expression measured by quantitative PCR, secretory activity did not differ significantly between proSP-C^{WT} and all mutant SP-C species analysed.

A549 cells process mutant proSP-C aberrantly and accumulate SP-C processing intermediates

To identify potential processing differences between pro-SP-C^{WT} and mutant proSP-C forms, we analysed proSP-C in A549 alveolar epithelial cells stably expressing N-terminally HA-tagged proSP-C^{WT}, proSP-C^{P30L}, proSP-C^{I73T}, proSP-C^{L110R}, proSP-C^{P115L}, proSP-C^{A116D} and proSP-C^{L188Q} by Western blotting. Expression of the N-terminally HA-tagged proSP-C^{WT} resulted in appearance of strong protein bands at approximately 21, 16 and 10 kDa (Fig. 1), thus resembling the pattern we previously reported for MLE-12 cells expressing HA-tagged proSP-C^{WT} [14]. A pattern similar to wild type was observed in proSP-C^{L110R}, while expression of proSP-C^{I73T}, proSP-C^{A116D} and proSP-C^{L188Q} yielded intense bands that

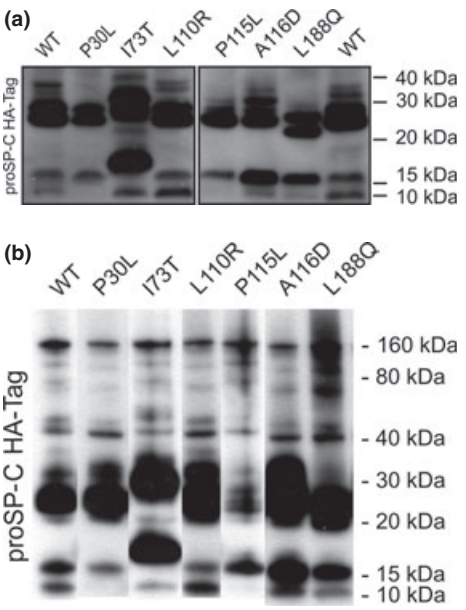

Figure 1 A549 cells process mutant proSP-C aberrantly and accumulate SP-C processing intermediates. Immunoblotting was performed using antibodies against the hemagglutinin (HA) tag for detection of proSP-C in cells expressing wild-type and mutant SP-C, respectively. In case of p.30L and p.P115L, no bands at 10 kDa could be detected. Aberrant bands were found in p.I73T, p.A116D and p.L188Q. (a) Blot was carried out using whole cell lysates. (b) Blot that was carried out after immunoprecipitation with HA beads for proSP-C purification.

were not seen in the wild type, indicating accumulation of misprocessed proSP-C. In contrast to these mutations and also to proSP-C^{WT}, neither proSP-C^{P30L} nor proSP-C^{P115L} yielded bands of < 16 kDa, indicating that processing was arrested at the 16-kDa stage.

Mutant proSP-C forms show altered intracellular distribution

The intracellular localization of proSP-C, monitored by immunofluorescence, differed between cells expressing proSP-C^{WT} and mutant proSP-C forms. ProSP-C^{WT} showed only little cytoplasmic background and a strong vesicular signal which colocalized with the lamellar body marker LAMP3/CD208 (Fig. 2b). Whereas proSP-C^{L110R} almost completely colocalized with LAMP3, similar to proSP-C^{WT}, the signals of proSP-C^{P30L}, proSP-C^{I73T}, proSP-C^{A116D} and proSP-C^{L188Q} were substantially less vesicular with a stronger cytoplasmic background. Pro-SP-C^{P115L} hardly colocalized with LAMP3. Dots showing colocalization of HA and LAMP3 were counted, and results were calculated as fraction of all HA dots (merge/HA) (Fig. 2c). The difference to wild type reached statistical significance in case of p.P30L and p.P115L. ($P < 0{\cdot}05$ and $P < 0{\cdot}001$, respectively). This indicates that mutant proSP-C is trafficked to LAMP3-positive vesicles to some extent, with the exception of proSP-C^{P115L}. In contrast to proSP-C^{WT}, proSP-C^{P30L}, proSP-C^{P115L} and proSP-C^{L188Q} colocalized with the ER marker calnexin (Fig. 2a). This suggests retention of proSP-C^{P30L}, proSP-C^{P115L} and proSP-C^{L188Q} in the ER. Two recent reports have suggested some extent of mistrafficking of proSP-C^{I73T} to the plasma membrane [23,30]. We performed immunofluorescence using nonpermeabilized cells to assess plasma membrane localization of proSP-C. From our results, we can confirm localization of SP-C^{I73T} (Fig. S1). Interestingly, similar albeit less pronounced plasma membrane localization was seen in proSP-C^{A116D} cells. However, in contrast to a recent study by Beers *et al.* [23], we did not find pronounced differences regarding endosomal localization of wild type and mutant proSP-C when using EEA1 as marker for early endosomes (Fig. S2). Likewise, no differences between wild type and mutant proSP-C were seen when we analysed colocalization with the Golgi marker GM130 (Fig. S3).

Stable expression of mutant SP-C is not associated with increased ER stress

It has previously been shown that SP-C mutations lead to an increase in ER stress [13,17]. An indicator of ER stress is the increased expression of ER resident chaperones like GRP78/BiP [31]. We therefore analysed BiP expression in A549 cells stably expressing proSP-C mutations. BiP expression was not changed in cells expressing proSP-C^{WT} or proSP-C^{L110R} when compared with nontransfected A549 cells (Fig. 3). In cells expressing proSP-C^{P30L}, proSP-C^{I73T}, proSP-C^{P115L}, pro-SP-C^{A116D} and proSP-C^{L188Q}, we found a reduced expression of BiP. Lowest BiP expression level was seen in proSP-C^{P115L} cells.

Mutant SP-C forms intracellular Congo red–positive aggregates

Congo red is a well-known marker for ß-sheet amyloid aggregates in numerous diseases, for example, in Alzheimer's disease [32]. Congo red staining revealed that proSP-C^{I73T} does not lead to aggregate formation as it is the case with proSP-C^{WT} (Fig. 4). In the case of proSP-C^{P30L} and proSP-C^{P115L} we detected strong intracellular Congo red–positive aggregates. Interestingly, proSP-C^{L110R} also formed ß-sheet aggregates as indicated by Congo red–positive aggregates. Other BRICHOS mutations, that is, p.A116D and p.L188Q, also resulted in the presence of Congo red–positive aggregates.

Mutant proSP-C is degraded by the ubiquitin–proteasome system while wild-type proSP-C enters the autophagocytosis pathway

In order to further assess the fate of misfolded proSP-C, we performed immune fluorescence analysis of ubiquitin. Wild-type proSP-C showed few dot-like signals and almost no colocalization with ubiquitin (Fig. 5a). In the case of proSP-C^{L110R}, there was also very little colocalization. In marked contrast, for proSP-C^{P30L}, proSP-C^{I73T}, proSP-C^{P115L}, proSP-C^{A116D} and proSP-C^{L188Q}, we observed significant colocalization of HA-tagged proSP-C with ubiquitin (Fig. 5b). Autophagocytic activity was assessed by immunoblotting using a LC3A/B antibody [33]. Lysates from cells expressing proSP-C^{WT} showed increased intensity of the lower LC3 band at 14 kDa when compared with untransfected cells, indicating increased autophagy in these cells (Fig. 5c). For proSP-C mutants, the band pattern resembled that of untransfecting cells, indicating unaltered autophagocytic activity. Taken together, mutant proSP-C forms enter ubiquitin-mediated degradation, while overexpression of SP-C^{WT} induces autophagy.

Discussion

While it has been recognized that mutations in the *SFTPC* gene are the basis of a significant proportion of genetically determined ILD, the mechanisms whereby mutations trigger these diseases are still far from clear. In stably transfected A549 cells, a cell line resembling alveolar type II cells in several important aspects, we characterized specific abnormalities of intracellular proSP-C trafficking and the fate of several mutant proSP-C species. All mutations in the *SFTPC* gene we investigated showed alterations of alveolar cell biology in comparison with SP-C^{WT}, whereas the cell viability was not impaired. Based on our results, we can distinguish a group of mutations (p.I73T,

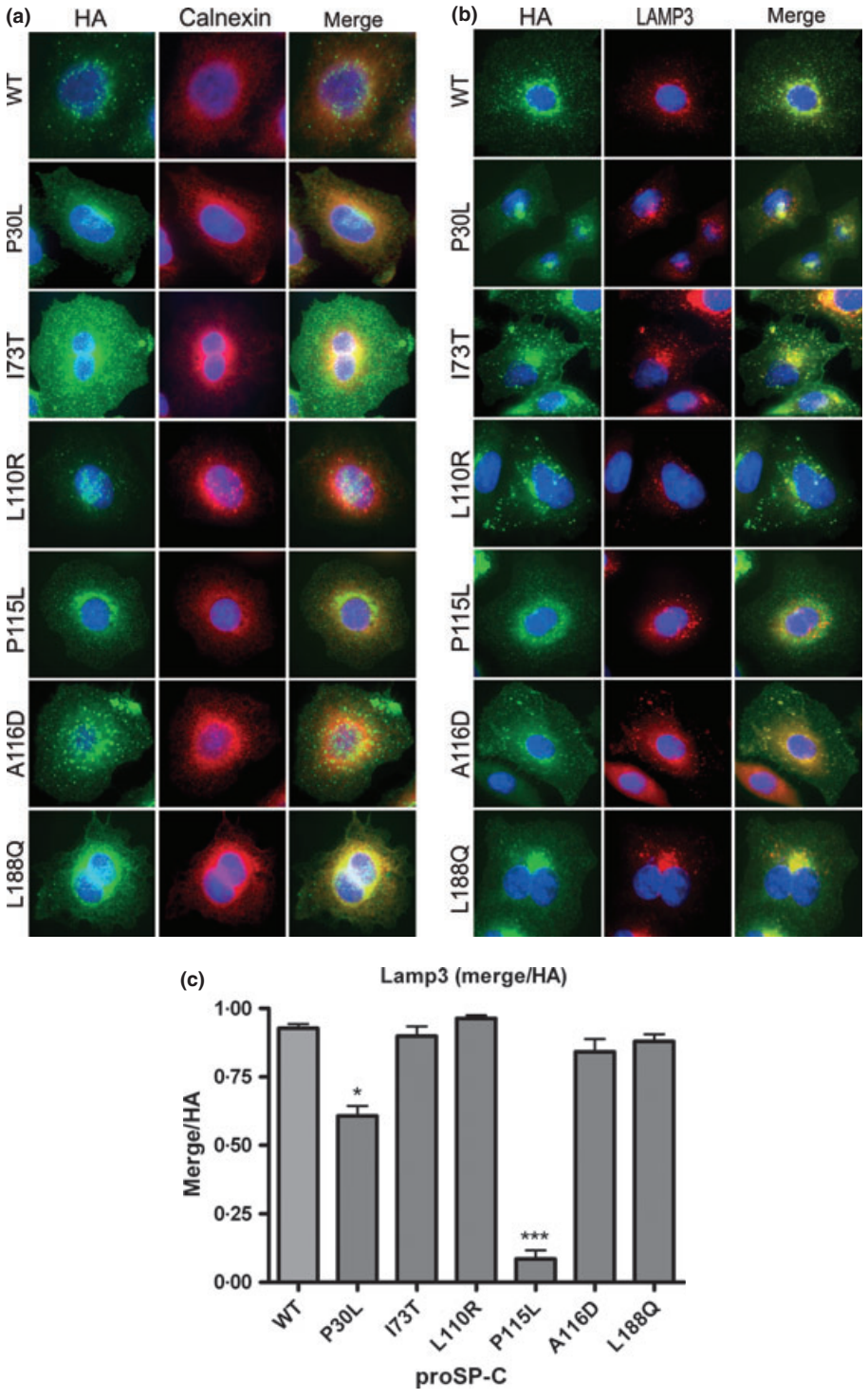

Figure 2 Mutant proSP-C forms show altered intracellular distribution. The intracellular localization and trafficking of proSP-C were analysed by fluorescence microscopy. Green channel: proSP-C visualized by hemagglutinin (HA) antibody. (a) Red channel: calnexin-positive structures, as a common marker for endoplasmic reticulum (ER); merge: overlapped green and red channel for the detection of colocalization between HA and calnexin. (b) LAMP3-positive vesicles are visualized in red channel by antibodies against LAMP3. LAMP3 is used as a marker for lysosomal structures, that is, lamellar bodies, which are important for proSP-C trafficking. Right side: green and right channel merged to visualize colocalization (yellow). Nuclei were visualized by DAPI (blue). (c) Dots showing colocalization of HA and LAMP3 were counted, and results were calculated as fraction of all HA dots (merge/HA). * $P < 0{\cdot}05$; *** $P < 0{\cdot}001$.

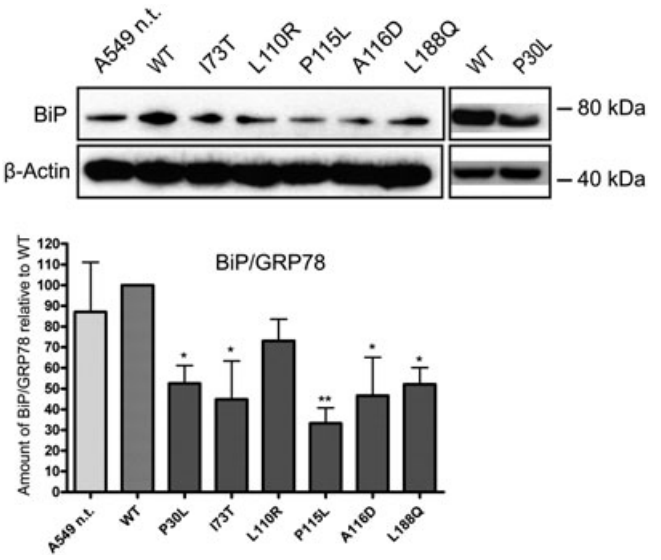

Figure 3 Stable expression of mutant proSP-C is not associated with increased ER stress. Semi-quantitative immunoblotting of cell lysates with antibody against BiP was performed. Protein expression was quantified by densitometry. BiP expression levels are given relative to proSP-C^{WT}. The difference to wild type reached statistical significance in all mutations investigated except for p.L110R. * $P < 0{\cdot}05$; ** $P < 0{\cdot}01$

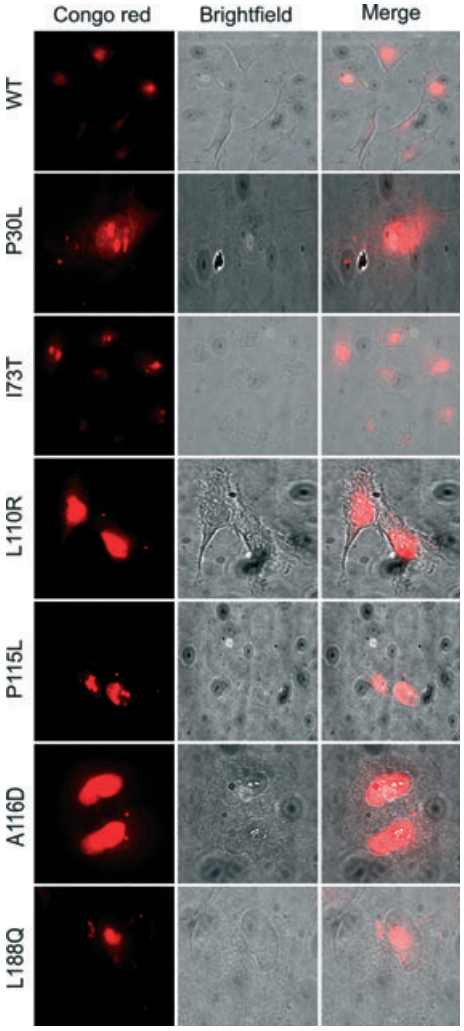

Figure 4 Certain proSP-C mutations lead to accumulation of intracellular Congo red–positive aggregates. Images from fluorescence microscopy at 555-nm emission after Congo red staining. For all BRICHOS mutations, intracellular aggregates were found. Also in the case of the non-BRICHOS mutation p.P30L mutation, some Congo red–positive aggregates were seen. proSP-C^{WT} and proSP-C^{I73T} did not show intracellular accumulation of Congo red–positive aggregates.

p.L110R, p.A116D and p.L188Q; partial lamellar body traffic) that result in aberrant proSP-C, which were at least partially trafficked to lamellar bodies, from another group of mutations (p.P30L and p.P115L; no lamellar body traffic) that do not enter the physiological pathway at all. The 'no lamellar body traffic' mutations induce ER arrest of the aberrant protein and inhibit further processing, as indicated by the absence of bands of < 16 kDa (Fig. 1). This is in concordance with our immunofluorescence studies that clearly demonstrate ER arrest of proSP-C with the mutations p.P30L and p.P115L (Fig. 2). Of interest, a feature observed in all mutations with the exception of p.I73T is the pronounced formation of Congo red–positive aggregates (Fig. 4). Thus, our data show that mutations localized in different domains of proSP-C may lead to very similarly impaired proSP-C processing.

Mutations with partial lamellar body traffic lead to proteins that are at least partly located to lamellar bodies. These proSP-C forms are correctly processed in the ER and routed into LAMP3-positive vesicles, that is, lamellar bodies, through which they could be subsequently secreted. This is in agreement with observations in bronchoalveolar lavages of infants with *SFTPC* mutations [4,19,34]. However, the intracellular effects of the mutations are different. While most of these mutations are aberrantly processed and result in intracellular accumulation of proSP-C, only proSP-C^{I73T} and proSP-C^{A116D} reach the plasma membrane via an alternative trafficking pathway [23,30]. p.L110R is the only mutation which does not induce increased degradation of proSP-C via the ubiquitin–proteasome system (Fig. 5a,b). ProSP-C^{L110R} behaves similar to proSP-C^{WT} in several aspects with the important exception that it forms intracellular Congo red–positive aggregates, like all BRICHOS mutants. Our data suggest that besides disturbed secretion, additional factors related to the intracellular traf-

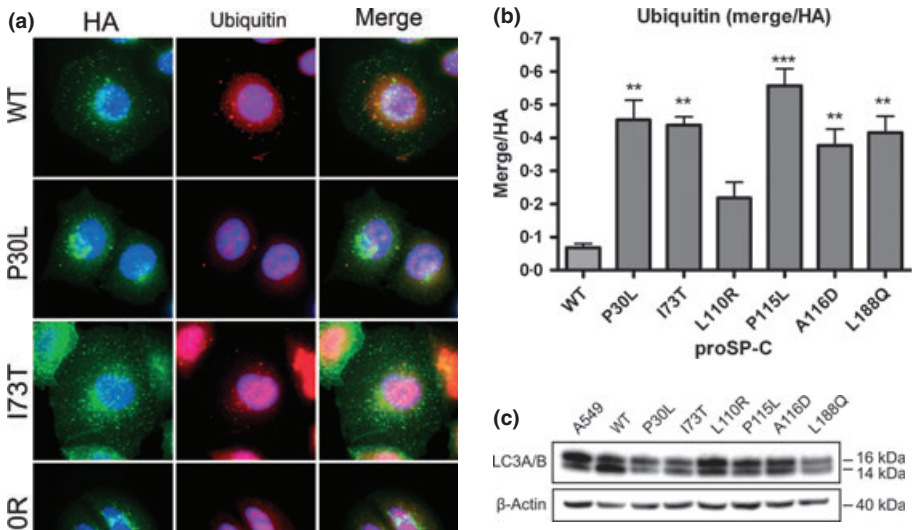

Figure 5 Mutant proSP-C is degraded by the ubiquitin–proteasome system, while wild-type proSP-C enters the autophagocytosis pathway. (a) Immunofluorescence microscopy was performed using antibodies against hemagglutinin (HA) tag (green channel) for detection of proSP-C and against ubiquitin (red channel). Right column shows both channels merged. For all proSP-C mutations except SP-C^{L110R}, colocalization of HA signal with ubiquitin can be seen, which indicates that proSP-C is being degraded in proteasomes. Nuclei were visualized by DAPI (blue). (b) Dots showing colocalization of HA and ubiquitin were counted, and results were calculated as fraction of all HA dots (merge/HA). The difference to wild type reached statistical significance in case of all proSP-C mutants except for p.L110R (** = $P < 0{\cdot}01$; *** = $P < 0{\cdot}001$). (c) To detect autophagy in proSP-C cells, immunoblotting was performed using antibody against LC3A/B. In contrast to SP-C mutants, wild-type proSP-C shows increased band at about 14 kDa, as a marker for upregulated autophagy. Same amounts of whole cell lysates were used.

ficking of proSP-C and its precursors have to be involved in the pathogenesis of ILD associated with mutations in *SFTPC*.

In apparent conflict with our results, previous studies conducted in cells transiently expressing SP-C mutations suggested a stress-induced up-regulation of BiP [13,16,31,35]. However, in such models, transfection itself poses a severe cellular stress, which is very likely to influence BiP levels for at least 48 h afterwards. Increased BiP levels may thus at least partly be attributable to cell stress related to transfection. Moreover, when using transient expression, cells are assayed for stress after only a few days. This period may be too short for cells to adapt to the ER stress induced by accumulation of mutant protein. In our model, cells are grown for several weeks and can thus compensate effects due to mutant protein expression. Adaption to chronic ER stress imposed by stable expression of the SP-C Δexon4 mutation has previously been demonstrated [36].

The BRICHOS domain of proSP-C has been described as critical for the correct post-translational processing of the protein [7]. Distinct mutations within this domain are believed to lead to similar consequences with regard to mistrafficking and intracellular accumulation of misfolded protein [7,16,37]. However, this assumption is not supported by our findings. Cells expressing SP-C^{L110R} did neither show ubiquitination nor show aberrant processing, and SP-C^{L110R} was properly localized in lamellar bodies. In marked contrast, SP-C^{P115L} did not reach lamellar bodies but is arrested in the ER. We suggest that in case of p.P115L, the replacement of proline, a so-called helix breaker, by leucine is likely to have more serious consequences for the conformation of the SP-C protein than the replacement of leucine by arginine in the case of p.L110R. To further support the notion that different BRICHOS mutations lead to distinct cellular consequences, we investigated two further BRICHOS domain mutations, namely p.A116D and

Table 1 Overview of results for all mutations investigated in this study

		Mutation					
		Mature	non-BRICHOS	BRICHOS			
Localization of mutation	**WT[a]**	**p.P30L**	**p.I73T**	**p.L110R**	**p.P115L**	**p.A116D**	**p.L188Q**
Feature							
Cell viability	Normal	Normal	Normal	Normal	Normal	Normal	Normal
Secretory capacity	Normal	Like WT	Like WT	Like WT	Like WT	Like WT	Like WT
Processing	Normal	No 10-kDa band	Aberrant bands	Resembling WT	No 10-kDa band	Aberrant bands	Aberrant bands
Trafficking to Golgi	Yes	Yes	Yes	Yes	Yes	Yes	Yes
Colocalization with calnexin	No	Yes	No	No	Yes	No	Yes
Trafficking to LB	Yes	Partially	Yes	Yes	No	Yes	Partially
Colocalization with LAMP3	Normal	Reduced	Normal	Normal	Reduced	Normal	Normal
BiP amount	Normal	Reduced	Reduced	Normal	Reduced	Reduced	Reduced
Congo red aggregates	No	Yes	No	Yes	Yes	Yes	Yes
Ubiquitination	No	Yes	Yes	No	Yes	Yes	Yes
Increased autophagy	Yes	No	No	No	No	No	No
Plasma membrane localization	No	No	Yes	No	No	Yes	No
Endosomal localization	To some extent	Like WT	Like WT	Like WT	Like WT	Like WT	Like WT

[a]Wild-type.

p.L188Q. These mutations also showed distinctly altered trafficking: while p.L188Q was mostly arrested in the ER, p.A116D appeared in lamellar bodies (Table 1). We conclude from the findings presented that not all BRICHOS domain mutations have similar consequences for proSP-C processing. Of interest, a common feature seen in all BRICHOS domain mutations was the formation of Congo red–positive aggregates. This is in line with the supposed role of the BRICHOS domain as an intramolecular chaperone that inhibits conformational changes of the transmembrane segment of proSP-C from α-helices to ß-sheet forms, that is, amyloid-like inclusions [8,24,37,38]. However, aggregate formation does not seem to be an exquisite characteristic of mutations affecting the BRICHOS domain because p.P30L, a non-BRICHOS domain mutation, also induced Congo red–positive intracellular aggregates. Normally, cysteine residues at positions 28 and 29 become palmitoylated during processing of proSP-C [7]. Correct interaction between palmitoylated cysteine and lipids stabilize the α-helix of the instable transmembrane domain [8,39]. Proline at position 30 is necessary for correct 3D-orientation of transmembrane domain. In case of p.P30L, this orientation could be disrupted because of replacement of proline by leucine [8,40]. As a consequence, the orientation of palmitoylated cysteines could be altered, causing the transmembrane domain to form Congo red–positive ß-fibrils.

In summary, our results demonstrate unique consequences of different proSP-C mutations for alveolar epithelial cell biology that are dependent on the actual residue altered. Intracellular trafficking and the fate of proSP-C cannot be predicted based on the localization of the actual mutation. Importantly, enhanced ER stress was not a general feature of the cells stably expressing mutated proSP-C. Our results strongly support the importance of studying single mutations in detail in order to develop specific therapies that target individual mutations or groups of mutations that share certain pathological features.

Acknowledgements

This study was supported by the Deutsche Forschungsgemeinschaft (DFG) Grants GR970-7.2 and GR970-7.3 to MG and

Grant 67/2008 by the University of Munich's Förderprogramm Forschung und Lehre to TT. This paper is part of the medical doctoral thesis of TT.

Authors' contributions

MG and SK conceived and designed the study as well as analysed and interpreted the data. TT, EK and RZ performed the experiments. RZ, MG and TT wrote the article.

Address

Dr. von Hauner Children's Hospital, Ludwig-Maximilians-University, Lindwurmstr. 4, 80337 Munich, Germany (T. Thurm, E. Kaltenborn, S. Kern, M. Griese, R. Zarbock).
Correspondence to: Matthias Griese, Children's Hospital of the Ludwig-Maximilians-University, Lindwurmstr. 4, D-80337 Munich, Germany. Tel.: +49-89-5160-7870; fax: +49-89-5160-7872; e-mail: Matthias.griese@med.uni-muenchen.de

Received 25 June 2012; accepted 21 April 2013

References

1 Baumgart F, Ospina OL, Mingarro I, Rodriguez-Crespo I, Perez-Gil J. Palmitoylation of pulmonary surfactant protein SP-C is critical for its functional cooperation with SP-B to sustain compression/expansion dynamics in cholesterol-containing surfactant films. *Biophys J* 2010;**99**:3234–43.
2 Johansson J. Structure and properties of surfactant protein C. *Biochim Biophys Acta* 1998;**1408**:161–72.
3 McAteer JA, Terracio L. Pulmonary type II cell lamellar body ultrastructure preserved by rapid freezing and freeze drying. *Anat Rec* 1984;**209**:355–62.
4 Beers MF, Kim CY, Dodia C, Fisher AB. Localization, synthesis, and processing of surfactant protein SP-C in rat lung analyzed by epitope-specific antipeptide antibodies. *J Biol Chem* 1994;**269**:20318–28.
5 Wang P, Chintagari NR, Narayanaperumal J, Ayalew S, Hartson S, Liu L. Proteomic analysis of lamellar bodies isolated from rat lungs. *BMC Cell Biol* 2008;**9**:34.
6 Kobayashi T, Vischer UM, Rosnoblet C, Lebrand C, Lindsay M, Parton RG *et al.* The tetraspanin CD63/lamp3 cycles between endocytic and secretory compartments in human endothelial cells. *Mol Biol Cell* 2000;**11**:1829–43.
7 Beers MF, Mulugeta S. Surfactant protein C biosynthesis and its emerging role in conformational lung disease. *Annu Rev Physiol* 2005;**67**:663–96.
8 Johansson J, Weaver TE, Tjernberg LO. Proteolytic generation and aggregation of peptides from transmembrane regions: lung surfactant protein C and amyloid beta-peptide. *Cell Mol Life Sci* 2004;**61**:326–35.
9 Nogee LM, Dunbar AE 3rd, Wert S, Askin F, Hamvas A, Whitsett JA. Mutations in the surfactant protein C gene associated with interstitial lung disease. *Chest* 2002;**121**(3 Suppl):20S–21S.
10 Thomas AQ, Lane K, Phillips J 3rd, Prince M, Markin C, Speer M *et al.* Heterozygosity for a surfactant protein C gene mutation associated with usual interstitial pneumonitis and cellular nonspecific interstitial pneumonitis in one kindred. *Am J Respir Crit Care Med* 2002;**165**:1322–8.
11 van Moorsel CH, van Oosterhout MF, Barlo NP, de Jong PA, van der Vis JJ, Ruven HJ *et al.* Surfactant protein C mutations are the basis of a significant portion of adult familial pulmonary fibrosis in a dutch cohort. *Am J Respir Crit Care Med* 2010;**182**:1419–25.
12 Cameron HS, Somaschini M, Carrera P, Hamvas A, Whitsett JA, Wert SE *et al.* A common mutation in the surfactant protein C gene associated with lung disease. *J Pediatr* 2005;**146**:370–5.
13 Maguire JA, Mulugeta S, Beers MF. Endoplasmic reticulum stress induced by surfactant protein C BRICHOS mutants promotes proinflammatory signaling by epithelial cells. *Am J Respir Cell Mol Biol* 2011;**44**:404–14.
14 Woischnik M, Sparr C, Kern S, Thurm T, Hector A, Hartl D *et al.* A non-BRICHOS surfactant protein c mutation disrupts epithelial cell function and intercellular signaling. *BMC Cell Biol* 2010;**11**:88.
15 Mulugeta S, Nguyen V, Russo SJ, Muniswamy M, Beers MF. A surfactant protein C precursor protein BRICHOS domain mutation causes endoplasmic reticulum stress, proteasome dysfunction, and caspase 3 activation. *Am J Respir Cell Mol Biol* 2005;**32**:521–30.
16 Mulugeta S, Maguire JA, Newitt JL, Russo SJ, Kotorashvili A, Beers MF. Misfolded BRICHOS SP-C mutant proteins induce apoptosis via caspase-4- and cytochrome c-related mechanisms. *Am J Physiol Lung Cell Mol Physiol* 2007;**293**:L720–9.
17 Lawson WE, Crossno PF, Polosukhin VV, Roldan J, Cheng DS, Lane KB *et al.* Endoplasmic reticulum stress in alveolar epithelial cells is prominent in IPF: association with altered surfactant protein processing and herpesvirus infection. *Am J Physiol Lung Cell Mol Physiol* 2008;**294**:L1119–26.
18 Stevens PA, Pettenazzo A, Brasch F, Mulugeta S, Baritussio A, Ochs M *et al.* Nonspecific interstitial pneumonia, alveolar proteinosis, and abnormal proprotein trafficking resulting from a spontaneous mutation in the surfactant protein C gene. *Pediatr Res* 2005;**57**:89–98.
19 Brasch F, Griese M, Tredano M, Johnen G, Ochs M, Rieger C *et al.* Interstitial lung disease in a baby with a de novo mutation in the SFTPC gene. *Eur Respir J* 2004;**24**:30–9.
20 Lawson WE, Grant SW, Ambrosini V, Womble KE, Dawson EP, Lane KB *et al.* Genetic mutations in surfactant protein C are a rare cause of sporadic cases of IPF. *Thorax* 2004;**59**:977–80.
21 Tredano M, Griese M, Brasch F, Schumacher S, de Blic J, Marque S *et al.* Mutation of SFTPC in infantile pulmonary alveolar proteinosis with or without fibrosing lung disease. *Am J Med Genet A* 2004;**126A**:18–26.
22 Hamvas A, Nogee L, White F, Schuler P, Hackett B, Huddleston C *et al.* Progressive lung disease and surfactant dysfunction with a deletion in surfactant protein C gene. *Am J Respir Cell Mol Biol* 2004;**30**:771–6.
23 Beers MF, Hawkins A, Maguire JA, Kotorashvili A, Zhao M, Newitt JL *et al.* A nonaggregating surfactant protein C mutant is misdirected to early endosomes and disrupts phospholipid recycling. *Traffic* 2011;**12**:1196–210.
24 Johansson H, Eriksson M, Nordling K, Presto J, Johansson J. The Brichos domain of prosurfactant protein C can hold and fold a transmembrane segment. *Protein Sci* 2009;**18**:1175–82.
25 Wang W. Deletion of exon 4 from human surfactant protein C results in aggresome formation and generation of a dominant negative. *J Cell Sci* 2002;**116**:683–92.
26 Bridges J, Wert S, Nogee L, Weaver T. Expression of a human surfactant protein C mutation associated with interstitial lung disease disrupts lung development in transgenic mice. *J Biol Chem* 2003;**278**:52739–46.

27 Rosen D, Waltz D. Hydroxychloroquine and surfactant protein C deficiency. *N Engl J Med* 2005;**352**:207–8.
28 Zarbock R, Woischnik M, Sparr C, Thurm T, Kern S, Kaltenborn E *et al*. The surfactant protein C mutation A116D alters cellular processing, stress tolerance, surfactant lipid composition, and immune cell activation. *BMC Pulm Med* 2012;**12**:15.
29 Weichert N, Kaltenborn E, Hector A, Woischnik M, Schams A, Holzinger A *et al*. Some ABCA3 mutations elevate ER stress and initiate apoptosis of lung epithelial cells. *Respir Res* 2011;**12**:4.
30 Stewart GA, Ridsdale R, Martin EP, Na CL, Xu Y, Mandapaka K *et al*. 4-Phenylbutyric acid treatment rescues trafficking and processing of a mutant surfactant protein-C. *Am J Respir Cell Mol Biol* 2012;**47**:324–31.
31 Zhang Y, Liu R, Ni M, Gill P, Lee AS. Cell surface relocalization of the endoplasmic reticulum chaperone and unfolded protein response regulator GRP78/BiP. *J Biol Chem* 2010;**285**:15065–75.
32 Giorgadze T, Shiina N, Baloch Z, Tomaszewski J, Gupta P. Improved detection of amyloid in fat pad aspiration: an evaluation of Congo red stain by fluorescent microscopy. *Diagn Cytopathol* 2004;**31**:300–6.
33 Tanida I, Waguri S. Measurement of autophagy in cells and tissues. *Methods Mol Biol* 2010;**648**:193–214.
34 Guillot L, Epaud R, Thouvenin G, Jonard L, Mohsni A, Couderc R *et al*. New surfactant protein C gene mutations associated with diffuse lung disease. *J Med Genet* 2009;**46**:490–4.
35 Zhong Q, Zhou B, Ann DK, Minoo P, Liu Y, Banfalvi A *et al*. Role of ER Stress in EMT of Alveolar Epithelial Cells: effects of Misfolded Surfactant Protein. *Am J Respir Cell Mol Biol* 2011;**45**:498–509.
36 Bridges J, Xu Y, Na C, Wong H, Weaver T. Adaptation and increased susceptibility to infection associated with constitutive expression of misfolded SP-C. *J Cell Biol* 2006;**172**:395–407.
37 Nerelius C, Gustafsson M, Nordling K, Larsson A, Johansson J. Anti-amyloid activity of the C-terminal domain of proSP-C against amyloid beta-peptide and medin. *Biochemistry* 2009;**48**:3778–86.
38 Nerelius C, Martin E, Peng S, Gustafsson M, Nordling K, Weaver T *et al*. Mutations linked to interstitial lung disease can abrogate anti-amyloid function of prosurfactant protein C. *Biochem J* 2008;**416**:201–9.
39 Willander H, Hermansson E, Johansson J, Presto J. BRICHOS domain associated with lung fibrosis, dementia and cancer–a chaperone that prevents amyloid fibril formation? *FEBS J* 2011;**278**:3893–904.
40 ten Brinke A, van Golde LM, Batenburg JJ. Palmitoylation and processing of the lipopeptide surfactant protein C. *Biochim Biophys Acta* 2002;**1583**:253–65.

Supporting Information

Additional Supporting Information may be found in the online version of this article:

Figure S1 ProSP-C^{I73T} and proSP-C^{A116D} enter the plasma membrane. Immunofluorescence microscopy with anti-HA antibody was performed in unpermeabilized cells to detect proSP-C in the plasma membrane. In case of proSP-C^{I73T} and proSP-C^{A116D}, the plasma membrane shows HA staining, indicating presence of proSP-C in the plasma membrane.

Figure S2 ProSP-C is localized in endosomal vesicles to some extent. The images show fluorescence microscopy was performed with antibodies against HA-tagged proSP-C (green channel) and EEA-1 (red channel), a marker for early endosomes. While some proSP-C can be seen in endosomal vesicles, no pronounced differences could be detected. Nucleoli were visualized by DAPI.

Figure S3 ProSP-C is trafficked to Golgi apparatus. Images show fluorescence microscopy was performed with antibodies against HA-tagged proSP-C (green channel) and GM130 (red channel), a commonly used marker for the Golgi apparatus, especially for cis-Golgi. Colocalization was observed for proSP-C^{WT} and also for proSP-C mutants. Nucleoli were visualized by DAPI.

